



Published in final edited form as:

Environ Sci Technol. 2020 August 04; 54(15): 9495–9509. doi:10.1021/acs.est.0c01655.

Impact of Hurricane Maria on Drinking Water Quality in Puerto Rico

Yishan Lin^{1,2}, Maria Sevillano Rivera¹, Tao Jiang¹, Guangyu Li¹, Irmarié Cotto¹, Solize Vosloo¹, Corey M.G. Carpenter², Philip Larese-Casanova¹, Roger W. Giese³, Damian E. Helbling², Ingrid Y. Padilla⁴, Zaira Rosario-Pabón⁵, Carmen Vélez Vega⁵, José F. Cordero⁶, Akram N. Alshwabkeh¹, Ameet Pinto¹, April Z. Gu^{*,2}

¹Department of Civil and Environmental Engineering, Northeastern University, Boston, MA

²School of Civil and Environmental Engineering, Cornell University, Ithaca, NY

³Department of Pharmaceutical Sciences, Northeastern University, Boston, MA

⁴Department of Civil Engineering and Surveying, University of Puerto Rico, Mayagüez, PR

⁵University of Puerto Rico – Medical Sciences Campus, San Juan, PR

⁶Department of Epidemiology and Biostatistics, University of Georgia, Athens, GA, USA

Abstract

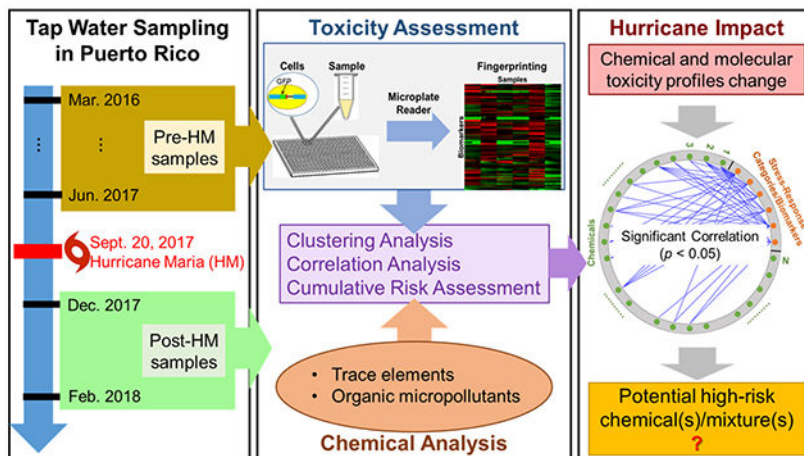
This study performed a comprehensive assessment of the impact of Hurricane Maria (HM) on drinking water quality in Puerto Rico (PR) by integrating targeted chemical analysis of both inorganic (18 trace elements) and organic trace pollutants (20 micropollutants) with high-throughput quantitative toxicogenomics and *in vitro* biomarkers-based toxicity assays. Average concentrations of 14 detected trace elements and 20 organic micropollutants showed elevation after HM. Arsenic, sucralose, perfluorooctanoic acid (PFOA), atrazine-2-hydroxy, benzotriazole, acesulfame, and prometon were at significantly ($p < 0.05$) higher levels in the post-HM than in the pre-HM samples. Thirteen micropollutants, including four pesticides, were only detected in post-hurricane samples. Spatial comparison showed higher pollutants and toxicity levels in the samples from northern PR (where eight Superfund sites are located) than in those from southern PR. Distinctive pathway-specific molecular toxicity fingerprints for water extracts before and after HM and at different locations revealed changes in toxicity nature that resulted likely from the impact of HM on drinking water composition. Correlation analysis and Maximum Cumulative Ratio assessment suggested that metals (i.e. arsenic) and PFOA were the top ranked pollutants that have the potential to cause increased risk after HM, providing a possible direction for future water resource management and epidemiological studies.

*Corresponding Author: aprilgu@cornell.edu, Tel: 607 255 8778; Fax: 607 255 9004.

SUPPORTING INFORMATION

Tap water sampling scheme, map distribution and ethics compliance; method description on elements and targeted organic micropollutants analyses; list of 74 proteins and data processing steps for toxicogenomics-based assay in yeast cells; maximum cumulative ratio (MCR) calculation; disease enrichment analysis using Comparative Toxicogenomics Database (CTD); concentration statistics of drinking water trace elements impacted by the hurricane and their spatial distribution; the primary usage and physicochemical properties of the detected organic micropollutants and their concentration statistics; Hurricane Maria impact on drinking water molecular toxicity levels/profiles based on the two toxicity assays and their spatial distribution; comparison of measured contaminant concentrations to human-health benchmarks.

Graphical Abstract



INTRODUCTION

On 20 September 2017, Hurricane Maria (HM) made direct landfall south of Yabucoa Harbor in Puerto Rico (PR) as a strong Category 4 storm, resulting in catastrophic flash floods and island-wide devastation.^{1, 2} HM directly killed 64 people in PR with excess deaths estimated from 990¹ to 4645³, destroyed over 90% of the electrical systems and 80% of the agricultural sectors, and left large areas without communication, water, and health care services, all of which resulted in an extremely slow post-hurricane recovery.^{1, 4} Limited studies on the impact of HM have reported increasing rates of adverse physical and psychological health consequences (e.g. fall-related injuries, leptospirosis infection, anxiety, post-traumatic stress)⁵⁻⁸ and hurricane-exacerbated environmental effects including persistent hydrological disruption,² deterioration of coastal water quality,⁹ increased air pollution,⁴ and disturbance of forest ecosystems.^{10, 11} However, little is known about the disruption of HM on drinking water quality that is critical to waterborne/water-related disease control and public health protection.¹²

Environmental pollution in PR was extensive even prior to HM, with over 200 hazardous waste sites including 18 active Superfund sites primarily contaminated by pesticides, chlorinated volatile organic compounds (CVOCs), and heavy metals.¹³ Recent studies have reported the HM-impaired regional water cycle and coastal waters in PR due to the disturbed land-surface vegetation and enhanced runoff,^{2, 9} which may trigger the release of various toxic substances into source waters and ultimately, degradation of drinking water quality when lack of effective water treatment systems.¹⁴ Initial investigation under the NIEHS Puerto Rico Test site for Exploring Contamination Threats (PROTECT) program suggested higher turbidity, bacteria counts, and concentrations of CVOCs, relative to water quality before HM.^{1, 14} Watkins et al. recently reported HM-related increases of urinary phthalate levels in the PR population,¹⁵ providing an evidence in hurricane-affected chemical exposures mostly via contaminated water and food sources. A recent water quality study focusing on microbial community characterization after two back-to-back hurricanes (Irma and Maria) on St. Thomas pointed out the urgent need for cistern water management to

prevent ingestion- and/or inhalation-related waterborne diseases.¹⁶ To our knowledge, post-disaster toxicological studies of drinking water for Hurricane Maria in PR have not yet been reported. Identities of the priority water pollutants that likely pose health risks due to HM are not yet clear.

Drinking water contains a large number of regulated and unregulated contaminants at trace levels from various environmental pollution sources and/or from water treatment processes,^{17–21} with known or unknown toxic effects on exposed human populations.^{22–24} Previous water quality surveys or disaster research often focused on individual or a single group of chemicals,^{15, 25, 26} which would not reflect the complexity and changing dynamics of chemical mixtures in drinking water supplies that may be exacerbated by hurricane events. Conventional resource-intensive animal-based and isolated bioassays targeting varying specific toxic effects at high doses may not meet the demands posed by disaster research which often requires timely response.^{27–29} Cost-effective and high throughput *in vitro* effect-based mixture toxicity evaluation methods, which can capture the multiple, diverse, and perhaps overlapping modes of action (MOA) resulting from trace-level water contaminant mixtures,^{30–33} are considered suitable for timely assessment of disaster impact on chemical exposure or whole water quality.²⁹ This study provide the first comprehensive evaluation of a hurricane's impact on drinking water quality and associated toxicity effects in PR by integrating wide-spectrum and targeted chemical analysis of both inorganic and organic trace pollutants with high-throughput quantitative toxicogenomics and *in vitro* biomarkers-based toxicity assays.^{34–37} Furthermore, correlation analysis and a cumulative risk assessment tool were further employed to probe the potential relationships between detected chemicals and environmental or human health outcome indicators. The outcome will contribute to our understanding of post-hurricane evolution and dynamics of complex contaminant mixtures in drinking water, providing timely yet informative results for initial toxicity screening and risk identification that can be potentially incorporated into the risk assessment and post-disaster water resource management strategy.

MATERIALS AND METHODS

Sampling Sites and Time

Two sampling schemes were introduced for tap water collection across PR before and after HM (Supporting Information, Part 1): (1) Sixteen tap water samples were collected in Northern PR from the households of participants recruited under the PROTECT program from April 2016 to June 2017, and they represented base-line condition before HM (designated as “B”). (2) Twenty tap water samples were collected post HM (designated as “P”) including eighteen samples from 9 locations across PR at two time points in December 2017 and February 2018, and two additional samples at Northern PR in February 2018. Note that the post-hurricane tap water sampling locations were different from the pre-HM locations because sampling at participants' households under the PROTECT program were impossible at the time due to the devastating conditions. Tap water samples were collected in a 5-liter pre-washed, baked amber glass jar with Teflon lid according to established standardized protocols^{38, 39} and ethics policies. Water samples were immediately transported

to the collaborating lab in the University of Puerto Rico on ice and were subjected to sample extraction within 24 hrs.

Sample Extraction and Preparation

For trace element analysis, raw tap water aliquots (20 mL each) were first filtered through a 0.45- μ m mixed cellulose ester membrane (Millipore) and then acidified with 0.5% HNO₃ (v/v). Organic compounds from tap water samples were enriched via a porous teabag extraction paddle (PEP) method on-site with deionized (DI) water as blank control, as described elsewhere.⁴⁰ The PEP assembly includes a wire mesh bag (Cat. # 3862, 25- μ m pore, Welch Fluorocarbon, Inc., USA) containing 1.0 g of Oasis HLB (60 μ m, Waters, MA, USA) that is anchored on a paddle in a 0.5-gallon glass jar (Industrial Glassware, NY, USA) where the raw tap water sample was continuously stirred at 190 rpm for ~16 hours per run. PEPs after sample extraction were dried and shipped to the lab at the Northeastern University (NU) under room temperature with Drierite Desiccant bags for elution and further analyses.

Sorbent in the PEP were eluted with acetonitrile (ACN) followed by methanol (MeOH), and the eluate was transferred into a sterile 5-ml cryogenic vial. The eluate was then blown dry using nitrogen gas, and re-dissolved in designated volume of sterile Milli-Q water, achieving an enrichment factor of 1400 times for the stock solution of tap water extract. Dilutions for the extracts were prepared using Milli-Q water for targeted organic analysis or phosphate buffer saline (PBS) for the two toxicity assays as described in later sections.

Trace Elements and Targeted Organic Micropollutants Analyses

A subset of the tap water samples (n = 21) was pre-acidified and analyzed for 18 trace elements (Supporting Information, Part 2) using inductively coupled plasma mass spectrometry (ICP-MS) method, including 10 samples before the hurricane and 11 samples after the hurricane (Figure S1).

Organic extracts from the 36 tap water samples were first diluted with Milli-Q water to achieve the final enrichment factor of 1000 times, filtered with 0.22- μ m polytetrafluoroethylene (PTFE) membrane (Fisher Scientific), and then subjected to target screening for 200 organic micropollutants (Table S2) by means of high-performance liquid chromatography (HPLC) coupled to high-resolution mass spectrometry (HRMS, quadrupole-orbitrap, Thermo Scientific).^{41, 42} These targeted chemicals include 13 PROTECT-relevant chemicals that were previously detected in water at PR⁴³ or in human subject samples⁴⁴⁻⁴⁶ and other emerging micropollutants often detected in surface waters around the world (Table S3). The analytical HPLC-HRMS method was previously developed and validated for a broad range of micropollutants,^{41, 42} details of which are summarized in the Supporting Information, and the target micropollutants and their limits of quantification (LOQ) are provided in Table S2.

Quantitative Toxicogenomics Assay

A quantitative toxicogenomics assay was employed to detect and quantify molecular-level changes in biomarker (protein) expression for fast, sensitive and mechanistic mixture

toxicity evaluation of tap water extracts.^{34–37} This assay employs a library of 74 yeast reporters with inframe green fluorescent protein (GFP)-fused biomarkers (Table S4) (Invitrogen, no. 95702, ATCC 201388), where the biomarker expression level was directly reflected by measured GFP signal.^{35–37, 47} The 74 biomarkers covered five key cellular stress response categories involved in general stress response, oxidative stress, protein stress, chemical stress and DNA stress.^{36, 37} Yeast cells share conserved strategies and stress responses with different eukaryotic cells^{48, 49} with substantial information available on gene function, and offer advantages over higher organisms, including being easy and fast to grow and store, low cost, and rapid response. These advantages make yeast a suitable testing platform for environmental applications with large numbers of samples.^{34–37, 50–52}

Due to the requirement of sub-cytotoxic exposure and the limitation of practical sample volume, we chose one dose of each tap water extract at relative enrichment factor (REF) of 200 for both yeast cell toxicogenomics-based and human cell biomarker-based assays. A detailed protocol for the toxicogenomics assay was previously described.^{34–37} In brief, the selected frozen yeast strains were seeded in SD medium with Dropout (DO) supplement-His (Clontech, CA, US) on a sterile clear bottom 384-well plate at 30 °C for 4–6 hours until the early exponential growth was reached. Tap water extract (REF=200) of 10 µL in PBS, blank control (SD medium + 0.25% YPD medium with or without chemical) or internal house-keeping control⁵³ (SD medium + 0.25% YPD medium + PGK1 strain with or without chemical) were added into the designated well. Plates were then placed in a Microplate Reader (Synergy TM H1 Multi-Mode, Biotech, Winooski, VT) for simultaneous cell growth (absorbance at 600 nm) and fluorescence (excitation at 485 nm, emission at 528 nm) measurements every 5 min for 2 hours after fast shaking (double orbital) for 1 minute. All tests were performed in dark in duplicate.

Detailed information on data processing was described previously (Supporting Information, Part 4).^{34–37} The molecular toxicity endpoint, Protein Effect Level Index (PELI), was calculated by integrating the temporal up-regulated induction factor (I) values over the exposure time. In this study, the assay cutoff threshold $PELI_{ORF}$ value of 1.5 was determined for differential gene expression in exposure to the tap water extract, on the basis of approximately 2 times the standard deviation for $PELI_{ORFi}$ in our yeast assay, as well as the threshold commonly used in previous toxicogenomics research.^{34, 36, 37, 54, 55}

Transcriptional Analysis of selected Biomarkers in Human A549 Cells

Reverse transcription quantitative PCR (RT-qPCR) technology was applied to quantify relative expression changes of 12 key biomarkers (genes) in human epithelial A549 lung cells involved in seven cellular stress and toxicity responses in exposure to the 34 tap water extracts (REF=200) for 6 hrs, including inflammation (*TNF-α*), apoptosis (*p53* and *Casp3*), oxidative damage (*HO1*), DNA damage (*Rad51* and *KU70*), chemical stress (*MTF-1*), endocrine disruption (*ESR2* and *AR*), and aryl hydrocarbon receptor (*AhR*, *CYP1A1*, and *CYP1B1*). No measurement was taken for 2 samples named BN1-QU and BN6-CI because of the limited sample volume. Detailed protocols were described previously.^{34, 36, 56} Exposed cells were subjected to RNA extraction using one-step RNA reagent (Bio Basic Inc., Canada), and reverse transcription to produce cDNA using Verso cDNA Synthesis Kit

(Thermo Fisher Scientific, US). Real-time quantitative PCR targeting the selected biomarkers was performed with SYBR® Green detection chemistry on iQ5 Multicolor Real-Time PCR detection system (Bio-Rad, CA). In this study, GAPDH was selected as internal control to normalize target gene quantities in each reaction.⁵⁷ The fold changes reflecting relative expression changes of targeted genes after sample treatment compared to an untreated calibrator control (all in triplicates), also referred to as induction factor *I*, were determined by the comparative C_T method (C_T method).⁵⁸

Maximum Cumulative Ratio (MCR) Calculation

To untangle toxicant interactions of complex mixtures, we applied the recently introduced maximum cumulative ratio (MCR) concept to identify potentially high-risk mixtures that may require further investigation, and the major chemicals possibly driving the cumulative risk in tap water samples.^{59–61} When calculating hazard quotient (HQ), permitted doses were selected as regulatory U.S. Environmental Protection Agency (USEPA) Maximum Contaminant Levels (MCLs) for regulated contaminants under the Safe Drinking Water Act (SDWA) or non-regulatory U.S. Geological Survey (USGS) Health-Based Screening Levels (HBSLs) for unregulated contaminants, when available. Details are described in the Supporting Information, Part 5.

Statistical Analysis

Mapping and geospatial analyses of chemicals and molecular toxicity levels were conducted in ArcGIS Desktop 10.2 (<http://resources.arcgis.com/en/help/main/10.2/index.html>). Concentrations of organic micropollutants were natural log transformed to more closely approximate a normal distribution. The Kolmogorov-Smirnov test was used to test data distribution pattern, and all chemical and toxicity data were standardized by creating z-scores to minimize the effects of varying chemical concentration and toxicity level differences at different sample sites.⁶² Unpaired t-test and Mann-Whitney U (MWU) test were then used to evaluate differences of chemical concentrations and toxicity responses between pre-hurricane samples and post-hurricane samples. Only the chemicals and toxic effects with $p < 0.05$ in both tests were considered as significantly changed after HM.

Hierarchical clustering analysis (HCA) was performed using correlation distance and average linkage as the distance measuring criteria, to group sampling sites with statistically similar protein expression patterns in yeast cells.⁶³ Correlation analysis was conducted to identify the potential association between molecular toxicity quantifiers and organic micropollutant concentrations detected in the tap water extracts using Pearson correlation ($p < 0.05$ as significant), assuming linear dose-response range of molecular toxicity effect at very low environmentally-relevant sub-cytotoxic levels as previously demonstrated.⁶⁴ Since toxicity assays were carried out on PEP-extracted samples with Oasis HLB sorbents that is mainly designed for sorptive preconcentration of organic compounds,^{65, 66} no correlation analysis was performed between molecular toxicity and inorganic trace elements. Finally, the Comparative Toxicogenomics Database (CTD) were used to test the input genes list associated with a target chemical for enrichment in diseases (details in Supporting Information, Part 6).^{67, 68}

RESULTS AND DISCUSSION

Impact of HM on Trace Element Levels in PR Drinking Water

Comparison of detected trace element levels in drinking water samples from PR before and after HM are shown in Figure 1a and Table S6. Eighteen trace elements were detected in tap water samples with frequencies ranging from about 19% to 100%, with their concentrations all below the MCLs or HBSLs (Table S6). Seven elements, including As, Ba, Cr, Cu, Fe, Pb, and Rb, were detected in all 21 tap water samples. The top 3 elements with highest average concentrations were Sr (160 µg/L), Cu (43 µg/L), and Ba (31 µg/L) (Figure 1a). Sixteen out of eighteen elements had elevated average concentration in the post-hurricane samples compared to those prior to HM, with Mn, Ni, As, and Cu exhibiting highest fold changes of 14.2, 3.5, 1.8 and 1.6 times (Table S6), respectively. According to both unpaired t-test and MWU test, contamination levels of arsenic in the tap water samples collected after HM were significantly higher than those before HM ($p < 0.05$), whereas concentrations of Ga and Th were significantly decreased after HM. As previously mentioned, the sampling locations before and after HM were not the same due to practical limitations. Recognizing that the 16 pre-HM samples were all from the Northern PR region, comparison analyses of chemical contamination levels for only Northern PR samples were also performed, which indicated similar overall trends in the elevation of pollutants after HM as for the entire PR island (Supporting Information, Part 10).

Cumulative concentrations of all detected trace elements and their distributions in each drinking water sample from different locations in PR are illustrated in Figure 2. Spatial comparison indicated higher cumulative trace element levels in the 17 samples collected from northern PR (where 8 active Superfund sites were located) than in the 4 samples collected at southern PR (other regions to the south of the PROTECT cohort, Figure 2). The highest cumulative element concentration was measured in the PN1-HA sample collected after HM on Dec. 18th, 2017 at Hatillo, PR, where ⁸⁸Sr contributed over 60% of the cumulative concentration (543 µg/L) (Figure 2). Storms and flooding brought about by HM could cause the releases of trace elements from air, soil, and/or sediments into the source waters, which might inadvertently be introduced into drinking water supplies. Our results indicated generally elevated trace element levels in the drinking water that are potentially associated with HM.

Impact of HM on Organic Micropollutants in PR Drinking Water

Targeted analysis was performed to detect 200 organic micropollutants (Table S2) in the 16 pre-HM samples and 20 post-HM samples.⁴¹ A summary of micropollutants detection frequencies and concentration statistics throughout the sampling scheme is provided in Table S8. Twenty-seven micropollutants (Table S7) were detected in at least one of the 36 samples, among which, 17 were wastewater-derived (including pharmaceutical and personal care products (PPCPs), plasticizers, perfluorochemicals, artificial sweeteners, etc.) and another 10 were agricultural-derived (pesticides) based on their primary uses.⁴¹ The top 5 micropollutants showing the highest occurrence frequency were N,N-diethyl-meta-toluamide (DEET, insect repellent), diethyl phthalate (DEP, plasticizer), benzophenone (PPCP), sucralose (artificial sweetener), and perfluorooctanoic acid (PFOA,

perfluorochemical) (Table S8). All micropollutants were measured within the 0.5 – 860 ng/L range and they were below the human-health benchmark levels (Table S11).

The temporal and spatial distribution of the organic micropollutants are shown in Figure 1b and Figure 2. Contamination levels of sucralose, PFOA, atrazine-2-hydroxy (atrazine degradation product), benzotriazole (ultraviolet stabilizer), acesulfame (sweetener), and prometon (herbicide) in the post-hurricane samples were significantly higher than in the pre-hurricane ones ($p < 0.05$). Generally, 22 out of the 27 detected micropollutants had higher detection frequencies in the 20 post-HM samples than in pre-hurricane samples, and 13 micropollutants, including 4 pesticides, were only detected in post-hurricane samples. Meanwhile, 20 out of the 27 micropollutants showed elevated average concentrations after HM with sucralose, atrazine-2-hydroxy, PFOA, and 2,4-dichlorophenoxyacetic acid (2,4-D) exhibiting the highest fold changes of 7.47, 3.64, 3.35, and 2.05, respectively (Figure 1b and Table S8). Figure 2 also shows a clear and consistent difference in the composition distribution of detected micropollutants with DEP and sucralose as the dominant component in pre-hurricane and post-hurricane samples, respectively. Close observation of chemical screening data for pre-hurricane samples revealed that 10 out of 14 detected organic micropollutants were only present in the samples collected during 2017 (Figure 2), demonstrating dynamic chemical contamination changes in PR even before HM from 2016 to 2017.

Similar to trace elements, average concentrations of the organic micropollutants showed a noticeable spatial pattern with overall higher concentrations in the tap water samples collected in northern PR than those in the southern PR samples (Figure 2). Higher detection frequencies were observed in the northern PR samples for 74% of the detected micropollutants. Seventeen (63%) micropollutants, including 8 pesticides, were only detected in the northern PR region.

For pesticide compounds, DEET, 2,4-D, and atrazine-2-hydroxy were among the top 10 most frequently detected micropollutants (Table S8), occurring in 100%, 47.2%, and 27.8% of all tap water samples, respectively. Among the 11 pesticides detected, occurrence of 7 pesticides was higher in the post-hurricane samples as compared to those collected before HM. DEET was detected in all 36 tap water extracts in the concentration range of 1.3 to 59.6 ng/L, which is higher than the detection frequency (25%) previously reported by USGS and the Centers for Disease Control and Prevention (CDC) in 2004⁶⁹ for finished drinking water samples in the US. DEET is the active ingredient of most commercial insect repellents, and its average usage in PR may be greater compared to the continental U.S. mainly due to greater prevalence of mosquito borne illness and monsoonal climates,⁷⁰ thus leading to higher detection frequency of DEET in the drinking water samples collected in PR. DEET was reported to have antagonistic interactions with cholinesterase and when used excessively, can cause some toxic side effects in humans including seizures⁷¹, Gulf War Syndrome⁷², and genotoxicity.⁷³

Hurricane Impact on Drinking Water Molecular Toxicity Profile

Toxicogenomics assay in yeast reporters—Distinctive stress response-related molecular toxicity profiles were revealed for tap water extracts retrieved before and after

HM and at different locations (Figure 3), demonstrating composition differences of tap water samples captured by the sensitive molecular toxicity assay, even at sub-cytotoxic doses. The molecular endpoint, PELI, derived from the yeast toxicogenomics assay allowed further quantitative comparison of the extent of molecular perturbation for each specific stress response category in exposure to the samples before and after HM (Table S9). Hierarchical clustering analysis reveals three major clusters that define groups of tap water samples inducing similar protein expression patterns in yeast cells (Figure 3). The first cluster contains 9 pre-hurricane samples that were collected in northern PR from March 2016 to June 2017 and 1 post-hurricane sample (Figure 3), inducing mainly up-regulation of biomarkers in protein and chemical stress. The second cluster includes 4 pre-hurricane samples collected in June 2017 and 1 post-hurricane sample from northern PR, showing stronger effect in oxidative stress. Meanwhile, 18 out of 20 tap water samples after HM were grouped together to form a third cluster, suggesting an impacting force (i.e. HM) covering the entire island (Figure 3).

The expression level of biomarkers related to oxidative stress (Skn7p regulation, glutathione biosynthesis) and protein stress (endoplasmic reticulum and mitochondrial unfolded protein response) were significantly different in the samples before and after HM ($p < 0.05$). A quantitatively higher extent of DNA damage in two specific pathways (DNA damage signaling, base excision repair) and stronger effect in three general stress pathways (apoptosis, osmotic stress, and trehalose synthesis) was detected for the post-hurricane samples compared to pre-hurricane ones (Table S9). In contrast, exposure to the pre-hurricane samples resulted in higher maximum PELI values in 24 out of 29 stress-response pathways primarily within chemical, protein, and oxidative stress categories (Table S9). These distinct molecular toxicity responses suggested the dynamic nature of toxicity resulting from co-exposure to varying contaminant mixtures in tap water extracts likely impacted by HM. It was noted that PELI values for all five stress categories and overall cellular stress response generally decreased for 8 out of 9 sampling sites from December 2017 to February 2018 (Figure S6a), indicating a possible temporal toxicity reduction trend of the water which needs further investigation by more extensive sampling.

RT-qPCR assay in Human biomarkers—Comparison of gene expression fold changes (I) for 12 biomarkers in human A549 cells in exposure to 14 samples collected before HM and 20 samples after HM were shown in Figure 4, Figure S6b and Table S10. Exposure to post-hurricane extracts induced significantly higher expression levels ($p < 0.05$) of *ESR2* and *TNF- α* genes, which are involved in endocrine disrupting (ED) and inflammation pathways, respectively, than those for pre-hurricane samples (Figure 4 and Table S10). Meanwhile, *Rad51* gene, assisting in DNA double-strand break repair (DSBR) mainly via homologous recombination (HR), exhibited significantly lower fold change levels in post-HM samples than pre-HM samples ($p < 0.05$).

Eight stress genes that are involved in six different cellular stress response pathways showed differential expression (fold change > 2 or < 0.5) relative to untreated control in at least one of the total 34 samples tested (Table S10). Noticeably, two genes, *CYP1A1* and *CYP1B1*, both in AHR pathway, showed differential up-regulation levels (fold change > 2) in 100% and 97% of all tap water samples, with higher expression levels in post-hurricane samples

compared to those prior to HM (Figure 4 and Table S10). Cytochrome P450s (CYPs), including CYP1A1 and CYP1B1, are essential heme-containing enzymes that were reported to be expressed in the human lung where they participate in metabolic inactivation and activation of numerous exogenous and endogenous compounds.^{74, 75} However, expression levels of the *AhR* gene, a ligand-activated transcriptional activator for the expression of multiple phase I and II xenobiotic chemical metabolizing enzyme genes, in all samples were comparatively low ($I = 0.67$ to 1.59) (Table S10), suggesting the possibility of the activation of the two CYP1 genes via alternative mechanisms other than AHR.⁷⁶

Higher molecular toxicity levels were detected in exposure to tap water collected at northern PR than southern as revealed by the two toxicity assays (Figure S7). In yeast cells, average expression levels of protein stress related to unfolded protein responses and autophagy to turn over misfolded or damaged proteins, was significantly higher for northern PR samples ($p < 0.05$) as compared with southern PR samples. In human cell assay, 46% of the northern PR samples exhibited averaged gene expression fold change across all biomarkers greater than 2, in contrast to only 25% of the samples collected at southern PR (Figure S7b). Exposure to northern PR samples mainly led to DNA damage, chemical stress and AHR stress, as indicated by the differential up-regulation (fold change > 2) of *Rad51*, *MTF-1*, and two genes in CYP1 family (Figure S6b). In contrast, exposure to the eight samples collected at other PR regions at the same concentration (REF=200) induced altered up-regulation of *TNF- α* (inflammation) and two CYP1 genes compared to the untreated control.

Correlation of Molecular Toxicity Quantifiers with Detected Contaminants

Pearson correlation was performed to investigate potential relationships between molecular toxicity quantifiers and organic micropollutant concentrations detected in the tap water extracts. Ten micropollutants were significantly correlated ($p < 0.05$) with the yeast-based stress response-relevant toxicity endpoints, while 17 were associated with expression changes of human biomarkers (Figure 5). The yeast toxicogenomics assay revealed quantitatively stronger DNA damage effect in two specific functional pathways after HM (Table S9), which showed significant correlation ($p < 0.05$) with caffeine (Figure 5a). Exposure to caffeine at environmentally-relevant concentrations (ng/L- μ g/L)⁷⁷ has previously shown to potentially induce genotoxic effects mainly through double-strand break and DNA repair inhibition in yeast cells, freshwater organisms and terrestrial insects.⁷⁸⁻⁸⁰ In our study, the correlation between the genotoxicity biomarkers with caffeine is therefore consistent with previous reports. However, since there was no significant difference in the caffeine levels in the samples obtained before and after HM, the stronger DNA damage effect observed in the post-hurricane samples was likely resulted from other DNA-damaging chemicals rather than caffeine. Meanwhile, benzoylecgonine (illicit drug metabolite), MCPA (herbicide) and temazepam (sedative drug), the three chemicals that were only detected in post-hurricane samples, showed significant correlation ($p < 0.05$) with *ESR2* gene in ED pathway (Figure 5b). Considering the significantly elevated expression level of this specific gene after HM (Figure 4 and Table S10), it is suggested that storms and flooding during HM may cause the subsequent releases of certain endocrine-disrupting chemicals (EDCs) potentially exhibiting increased ED activity in the aftermath of HM.

The targeted chemical analysis revealed statistically significant ($p < 0.05$) elevation of sucralose, PFOA, atrazine-2-hydroxy, benzotriazole, acesulfame, and prometon after HM (Figure 1b and Table S8). According to Pearson's correlation, PFOA was significantly correlated ($p < 0.05$) with chemical and oxidative stress categories in yeast cells (Figure 5a), and DNA damage (*Rad51*) in human A549 cells (Figure 5b). PFOA, at concentrations within and/or beyond that found environmentally, has been previously reported to induce oxidative stress by stimulating intracellular reactive oxygen species (ROS) production^{81–83}, which may cause indirect oxidative DNA damage including DNA strand breaks^{84–86} and may develop to mutagenicity under the condition where PFOA-induced apoptosis is not sufficient to remove damaged cells.⁸⁶ Acesulfame, a globally-used no-sugar or low-calorie sweetener, has been recently listed as an emerging contaminant due to its wide occurrence and persistence in the environment, mostly in water bodies.^{87–89} Our results showed that acesulfame, together with another artificial sweetener—sucralose, were both significantly correlated ($p < 0.05$) with oxidative stress in yeast cells and *CYP1B1* gene in human cells (Figure 5). Limited ecotoxicological data suggested that exposure to the two sweeteners, either at environmentally-relevant concentrations or at higher doses, may induce oxidative stress in different target species such as *Cyprinus carpio*,^{90, 91} zebrafish embryo,⁹² or *Daphnia magna*⁹³.

Maximum Cumulative Ratio (MCR) Approach Reveals Potential Cumulative Risk Drivers

Because of the growing concern on the potential mixture effects of multiple contaminants, a tiered approach integrating the MCR concept has been applied in this study to further probe the potential risk driver(s).^{61, 94} Human-health benchmarks were available for 29 of the 45 contaminants (18 trace elements and 27 organic micropollutants) detected in PR drinking water samples (Table 1 and S11). The other 16 contaminants without benchmarks, including 12 organic contaminants and 4 trace elements, were excluded from this analysis. The concentrations of the 29 detected contaminants with human-health benchmarks were below their corresponding guideline levels ($HQ < 1$, Table S11); among them, 3 contaminants (As, Fe, and Cu) had detected concentrations greater than one-tenth of their human-health benchmarks ($0.1 < HQ < 1$) in at least one of the 21 samples. Further monitoring to analyze trends in their occurrence, and to evaluate their potency (which may approach or exceed human-health benchmarks) may be needed for preventive actions on source control.^{95, 96}

For mixture risk analysis of different samples based on the hazard index (HI) (Part 5, Supporting Information) and MCR values, HI is < 1 in about 90% of the samples (all 10 pre-hurricane samples and 9 out of 11 post-hurricane samples), indicating low or no concern for potential cumulative adverse effects to tap water consumers from these 29 contaminants present in the mixture (group II, Table S5). Only 2 samples collected after HM at the municipalities of Manati and Cayey, fall into the group IIIA, where HI is > 1 and $MCR < 2$, indicating the majority of the identified potential risk offered by the mixtures may be driven by one dominant contaminant (Table 1). In addition, chemical components with benchmarks have been ranked according to their HQ values, and the top five high-priority substances in different mixtures were listed in Table 1. It was shown that nine naturally occurring trace elements (As, Fe, Cu, Sr, Pb, Ba, Zn, Ni, and Al) and one radionuclide (U) accounted for 80% to 100% of the top five predominant contaminants in all tap water samples collected in

PR. Starting from 1983, seven contaminated sites across PR have been listed as Superfund sites due to releases of metals such as Hg, As, Pb, Cd, Cr, and Mn, primarily from runoff from industrial or landfill wastes, and/or discharge of drilling wastes and metal refineries.¹³ Particularly, arsenic was the top-prioritized contaminant in all samples with HQ values ranging from 0.17 (in sample BN10 before HM) to 0.99 (in PN1-MN after HM), with contamination levels significantly higher ($p < 0.05$) in the post-hurricane samples than the pre-hurricane samples. Enrichment analysis using the CTD⁶⁸ revealed that arsenic exposure may selectively enrich (corrected p -value < 0.05) a total of 642 different diseases including 138 “cancer” diseases, 96 nervous system diseases, 60 digestive system diseases, 54 cardiovascular diseases, 41 immune system diseases, etc., in human, mouse and/or rat.

PFOA, which was elevated in post-hurricane samples, was the only organic contaminant that has been ranked as a top-five contaminant in 6 of the 21 samples including 1 pre-hurricane and 5 post-hurricane samples. PFOA has been previously reported to be detected in drinking water supplies, typically associated with industrial manufacturing and through use and disposal of PFAS-containing products.⁹⁷ Due to its high solubility in water and high resistance to degradation, the wide distribution, mobility, and toxicity of PFOA results in the potential for several adverse effects to human health under different exposure scenarios.^{97, 98} Based on the CTD screening, a total of 598 diseases were selectively enriched by PFOA exposure with the top 5 ranked diseases in the categories of “digestive system diseases” (MESH: D004066 and D008107), “cancer” (MESH: D009369 and D009371), and a nutritional and metabolic disease (MESH: D009750).

Overall, drinking water in PR showed different contamination levels before and after HM with clear spatial patterns for both trace elements and organic micropollutants. Both chemical composition analysis and toxicity fingerprints evaluation suggested that Hurricane Maria likely affected drinking water quality in PR, with the recognition of other impacting factors (i.e. background spatial and temporal changes in water sources). However, note that all the observed chemical contamination levels for both pre-HM and post-HM samples were well below their corresponding health-based guideline levels. Moreover, the toxicity assays were performed at enriched concentrations (REF = 200) with the purpose to identify potential adverse effects at the molecular level and the results cannot be directly translated into health outcomes. Although lack of human-health benchmarks for many of the detected contaminants prevents the MCR analysis from including all detected contaminants, the exercise suggested that the chemicals that potentially drive the cumulative risk in drinking water were mostly trace metals, pointing out a direction for post-disaster source control and water treatment process management in PR. Our combined approach of targeted chemical analysis and high-throughput toxicogenomics-based assay provides a feasible and efficient alternative for time-sensitive research such as post-disaster effect-based water quality monitoring, providing bases for further investigation of associated potential health risks and outcomes. Efforts are still on-going for continuous monitoring of the drinking water quality and toxicity after HM in PR, aiming to gain understanding of potential long-term impact of hurricanes on water quality and associated human and environmental health.

Supplementary Material

Refer to Web version on PubMed Central for supplementary material.

ACKNOWLEDGEMENTS

This study is supported by the United States National Science Foundation (NSF, CBET-1829754, CBET-1832756, IIS-1546428), the National Institute of Environmental Health Sciences (NIEHS) grants P42ES017198 and P50ES026049, and Assistance Agreement Number 83615501 from the U.S. Environmental Protection Agency (EPA).

REFERENCE

1. Brown P; Vega CMV; Murphy CB; Welton M; Torres H; Rosario Z; Alshawabkeh A; Cordero JF; Padilla IY; Meeker JD, Hurricanes and the Environmental Justice Island: Irma and Maria in Puerto Rico. *Environmental Justice* 2018, 11, (4), 148–153. [PubMed: 31131071]
2. Miller P; Kumar A; Mote T; Moraes F; Mishra D, Persistent Hydrological Consequences of Hurricane Maria in Puerto Rico. *Geophysical Research Letters* 2019, 46, (3), 1413–1422.
3. Kishore N; Marqués D; Mahmud A; Kiang MV; Rodríguez I; Fuller A; Ebner P; Sorensen C; Racy F; Lemery J, Mortality in puerto rico after hurricane maria. *New England Journal of Medicine* 2018, 379, (2), 162–170.
4. Subramanian R; Ellis A; Torres-Delgado E; Tanzer R; Malings C; Rivera F; Morales M; Baumgardner D; Presto A; Mayol-Bracero OL, Air quality in puerto rico in the aftermath of hurricane maria: a case study on the use of lower cost air quality monitors. *ACS Earth and Space Chemistry* 2018, 2, (11), 1179–1186.
5. Ferré IM; Negrón S; Shultz JM; Schwartz SJ; Kossin JP; Pantin H, Hurricane Maria's Impact on Punta Santiago, Puerto Rico: Community Needs and Mental Health Assessment Six Months Postimpact. *Disaster Medicine and Public Health Preparedness* 2019, 13, (1), 18–23. [PubMed: 30394256]
6. Orengo-Aguayo R; Stewart RW; de Arellano MA; Suárez-Kindy JL; Young J, Disaster exposure and mental health among Puerto Rican youths after Hurricane Maria. *JAMA Network Open* 2019, 2, (4), e192619–e192619. [PubMed: 31026024]
7. Ramírez-Martínez L; Chamah-Nicolás M; Nieves-Plaza M; Ruiz-Rodríguez J; Ruiz-Medina P; Ramos-Melendez EO; Rodríguez-Ortiz P, Epidemiology of traumatic falls after Hurricane Maria in Puerto Rico. *Injury Epidemiology* 2020, 7, (1), 19. [PubMed: 32475351]
8. Scaramutti C; Salas-Wright CP; Vos SR; Schwartz SJ, The Mental Health Impact of Hurricane Maria on Puerto Ricans in Puerto Rico and Florida. *Disaster Medicine and Public Health Preparedness* 2019, 13, (1), 24–27. [PubMed: 30696508]
9. Hernandez WJ; Ortiz-Rosa S; Armstrong RA; Geiger EF; Eakin CM; Warner RA, Quantifying the Effects of Hurricanes Irma and Maria on Coastal Water Quality in Puerto Rico using Moderate Resolution Satellite Sensors. *Remote Sensing* 2020, 12, (6), 15.
10. Eppinga MB; Pucko CA, The impact of hurricanes Irma and Maria on the forest ecosystems of Saba and St. Eustatius, northern Caribbean. *Biotropica* 2018, 50, (5), 723–728.
11. Lloyd JD; Rimmer CC; Salguero-Faría JA, Short-term effects of hurricanes Maria and Irma on forest birds of Puerto Rico. *PloS One* 2019, 14, (6), e0214432. [PubMed: 31185024]
12. Cook A; Watson J; van Buynder P; Robertson A; Weinstein P, 10th Anniversary Review: Natural disasters and their long-term impacts on the health of communities. *Journal of Environmental Monitoring* 2008, 10, (2), 167–175.
13. United States Environmental Protection Agency, Superfund: National Priorities List (NPL) homepage. <https://www.epa.gov/superfund/superfund-national-priorities-list-npl> (8 10, 2019),
14. Reardon S, Puerto Rico struggles to assess hurricane's health effects. *Nature News* 2017, 551, (7680), 282.
15. Watkins DJ; Torres Zayas HR; Vélez Vega CM; Rosario Z; Welton M; Agosto Arroyo LD; Cardona N; Díaz Reguero ZJ; Santos Rivera A; Huerta-Montañez G; Brown P; Alshawabkeh A;

- Cordero JF; Meeker JD, Investigating the impact of Hurricane Maria on an ongoing birth cohort in Puerto Rico. *Population and Environment* 2020.
16. Jiang SC; Han M; Chandrasekaran S; Fang Y; Kellogg CA, Assessing the water quality impacts of two Category-5 hurricanes on St. Thomas, Virgin Islands. *Water Research* 2020, 171, 115440. [PubMed: 31955059]
 17. Fang W; Peng Y; Muir D; Lin J; Zhang X, A critical review of synthetic chemicals in surface waters of the US, the EU and China. *Environment International* 2019, 131, 104994. [PubMed: 31302480]
 18. Richardson SD; Ternes TA, Water analysis: emerging contaminants and current issues. *Analytical Chemistry* 2017, 90, (1), 398–428. [PubMed: 29112806]
 19. Schwarzenbach RP; Escher BI; Fenner K; Hofstetter TB; Johnson CA; Von Gunten U; Wehrli B, The challenge of micropollutants in aquatic systems. *Science* 2006, 313, (5790), 1072–1077. [PubMed: 16931750]
 20. Sedlak DL; Gray JL; Pinkston KE, Peer reviewed: Understanding microcontaminants in recycled water. *Environmental Science & Technology* 2000, 34, (23), 508A–515A.
 21. Stehle S; Schulz R, Agricultural insecticides threaten surface waters at the global scale. *Proceedings of the National Academy of Sciences* 2015, 112, (18), 5750–5755.
 22. Murray KE; Thomas SM; Bodour AA, Prioritizing research for trace pollutants and emerging contaminants in the freshwater environment. *Environmental Pollution* 2010, 158, (12), 3462–3471. [PubMed: 20828905]
 23. Pal A; Gin KY-H; Lin AY-C; Reinhard M, Impacts of emerging organic contaminants on freshwater resources: review of recent occurrences, sources, fate and effects. *Science of the total environment* 2010, 408, (24), 6062–6069.
 24. Richardson SD; Plewa MJ; Wagner ED; Schoeny R; DeMarini DM, Occurrence, genotoxicity, and carcinogenicity of regulated and emerging disinfection by-products in drinking water: a review and roadmap for research. *Mutation Research/Reviews in Mutation Research* 2007, 636, (1–3), 178–242.
 25. Moschet C; Gotz C; Longree P; Hollender J; Singer H, Multi-level approach for the integrated assessment of polar organic micropollutants in an international lake catchment: the example of Lake Constance. *Environ Sci Technol* 2013, 47, (13), 7028–36. [PubMed: 23441970]
 26. Moschet C; Wittmer I; Simovic J; Junghans M; Piazzoli A; Singer H; Stamm C; Leu C; Hollender J, How a complete pesticide screening changes the assessment of surface water quality. *Environ Sci Technol* 2014, 48, (10), 5423–32. [PubMed: 24821647]
 27. (NIEHS), N. I. o. E. H. S. Science-ready - enabling public health research during disasters. https://factor.niehs.nih.gov/spotlight-disasters:file721380_alt
 28. (NIEHS), N. I. o. E. H. S. Rapid Acquisition of Pre- and Post-Incident Disaster Data Study. <https://clinicaltrials.gov/ct2/show/NCT02473770>
 29. (NIEHS), N. I. o. E. H. S. Oil Spill Response and Research. https://www.niehs.nih.gov/health/materials/oil_spill_response_and_research_508.pdf
 30. Brack W; Ait-Aissa S; Burgess RM; Busch W; Creusot N; Di Paolo C; Escher BI; Mark Hewitt L; Hilscherova K; Hollender J; Hollert H; Jonker W; Kool J; Lamoree M; Muschket M; Neumann S; Rostkowski P; Ruttkies C; Schollee J; Schymanski EL; Schulze T; Seiler T-B; Tindall AJ; De Aragão Umbuzeiro G; Vrana B; Krauss M, Effect-directed analysis supporting monitoring of aquatic environments — An in-depth overview. *Science of The Total Environment* 2016, 544, 1073–1118.
 31. Carpenter DO; Arcaro K; Spink DC, Understanding the human health effects of chemical mixtures. *Environmental Health Perspectives* 2002, 110, (suppl 1), 25–42. [PubMed: 11834461]
 32. Neale PA; Antony A; Bartkow ME; Farre MJ; Heitz A; Kristiana I; Tang JY; Escher BI, Bioanalytical assessment of the formation of disinfection byproducts in a drinking water treatment plant. *Environmental Science & Technology* 2012, 46, (18), 10317–10325. [PubMed: 22873573]
 33. Tang JY; Escher BI, Realistic environmental mixtures of micropollutants in surface, drinking, and recycled water: herbicides dominate the mixture toxicity toward algae. *Environmental Toxicology and Chemistry* 2014, 33, (6), 1427–1436. [PubMed: 24648273]

34. Lan J; Gou N; Gao C; He M; Gu A, Comparative and Mechanistic Genotoxicity Assessment of Nanomaterials via A Quantitative Toxicogenomics Approach Across Multiple Species. *Environmental Science & Technology* 2014, 48, (21), 12937–45. [PubMed: 25338269]
35. Lan J; Gou N; Rahman SM; Gao C; He M; Gu AZ, A quantitative toxicogenomics assay for high-throughput and mechanistic genotoxicity assessment and screening of environmental pollutants. *Environmental science & technology* 2016, 50, (6), 3202–3214. [PubMed: 26855253]
36. Lan J; Hu M; Gao C; Alshwabkeh A; Gu AZ, Toxicity Assessment of 4-Methyl-1-cyclohexanemethanol and Its Metabolites in Response to a Recent Chemical Spill in West Virginia, USA. *Environmental Science & Technology* 2015, 49, (10), 6284–6293. [PubMed: 25961958]
37. O'Connor STF; Lan J; North M; Loguinov A; Zhang L; Smith MT; Gu AZ; Vulpe C, Genome-wide functional and stress response profiling reveals toxic mechanism and genes required for tolerance to benzo [a] pyrene in *S. cerevisiae*. *Frontiers in genetics* 2012, 3, 316. [PubMed: 23403841]
38. EPA U, Quick Guide To Drinking Water Sample Collection. In USR Laboratory and Editors: 2005.
39. Munch DJ; Hautman DP, Method 551.1: Determination of chlorination disinfection byproducts, chlorinated solvents, and halogenated pesticides/herbicides in drinking water by liquid-liquid extraction and gas chromatography with electron-capture detection. *Methods for the Determination of Organic Compounds in Drinking Water* 1995.
40. Shao G; MacNeil M; Yao Y; Giese RW, Porous extraction paddle: a solid- phase extraction technique for studying the urine metabolome. *Rapid Communications in Mass Spectrometry* 2016, 30, (23), 2462–2470. [PubMed: 27624170]
41. Carpenter CM; Helbling DE, Widespread micropollutant monitoring in the Hudson River Estuary reveals spatiotemporal micropollutant clusters and their sources. *Environmental Science & Technology* 2018, 52, (11), 6187–6196. [PubMed: 29742349]
42. Gao H; LaVergne JM; Carpenter CMG; Desai R; Zhang X; Gray K; Helbling DE; Wells GF, Exploring co-occurrence patterns between organic micropollutants and bacterial community structure in a mixed-use watershed. *Environmental science. Processes & impacts* 2019, 21, (5), 867–880. [PubMed: 30957808]
43. Kalhor K; Ghasemizadeh R; Rajic L; Alshwabkeh A, Assessment of groundwater quality and remediation in karst aquifers: A review. *Groundwater for Sustainable Development* 2019, 8, 104–121. [PubMed: 30555889]
44. Meeker JD; Cantonwine DE; Rivera-González LO; Ferguson KK; Mukherjee B; Calafat AM; Ye X; Anzalota Del Toro LV; Crespo-Hernández N; Jiménez-Vélez B; Alshwabkeh AN; Cordero JF, Distribution, variability, and predictors of urinary concentrations of phenols and parabens among pregnant women in Puerto Rico. *Environmental science & technology* 2013, 47, (7), 3439–3447. [PubMed: 23469879]
45. Ferguson KK; Rosen EM; Rosario Z; Feric Z; Calafat AM; McElrath TF; Vélez Vega C; Cordero JF; Alshwabkeh A; Meeker JD, Environmental phthalate exposure and preterm birth in the PROTECT birth cohort. *Environment International* 2019, 132, 105099. [PubMed: 31430608]
46. Watkins DJ; Vélez-Vega CM; Rosario Z; Cordero JF; Alshwabkeh AN; Meeker JD, Preliminary assessment of exposure to persistent organic pollutants among pregnant women in Puerto Rico. *International journal of hygiene and environmental health* 2019, 222, (2), 327–331. [PubMed: 30738742]
47. Huh W-K; Falvo JV; Gerke LC; Carroll AS; Howson RW; Weissman JS; O'Shea EK, Global analysis of protein localization in budding yeast. *Nature* 2003, 425, (6959), 686. [PubMed: 14562095]
48. Liu XD; Liu PC; Santoro N; Thiele DJ, Conservation of a stress response: human heat shock transcription factors functionally substitute for yeast HSF. *The EMBO journal* 1997, 16, (21), 6466–77. [PubMed: 9351828]
49. Rodrigues-Pousada CA; Nevitt T; Menezes R; Azevedo D; Pereira J; Amaral C, Yeast activator proteins and stress response: an overview. *FEBS letters* 2004, 567, (1), 80–5. [PubMed: 15165897]

50. Daunert S; Barrett G; Feliciano JS; Shetty RS; Shrestha S; Smith-Spencer W, Genetically engineered whole-cell sensing systems: coupling biological recognition with reporter genes. *Chemical reviews* 2000, 100, (7), 2705–38. [PubMed: 11749302]
51. Estruch F, Stress-controlled transcription factors, stress-induced genes and stress tolerance in budding yeast. *FEMS microbiology reviews* 2000, 24, (4), 469–86. [PubMed: 10978547]
52. Yagi K, Applications of whole-cell bacterial sensors in biotechnology and environmental science. *Applied microbiology and biotechnology* 2007, 73, (6), 1251–8. [PubMed: 17111136]
53. Nakatani Y; Yamada R; Ogino C; Kondo A, Synergetic effect of yeast cell-surface expression of cellulase and expansin-like protein on direct ethanol production from cellulose. *Microbial cell factories* 2013, 12, (1), 66. [PubMed: 23835302]
54. Gou N; Onnis-Hayden A; Gu AZ, Mechanistic toxicity assessment of nanomaterials by whole-cell-array stress genes expression analysis. *Environmental Science & Technology* 2010, 44, (15), 5964–5970. [PubMed: 20586443]
55. McCarthy DJ; Smyth GK, Testing significance relative to a fold-change threshold is a TREAT. *Bioinformatics* 2009, 25, (6), 765–771. [PubMed: 19176553]
56. Khatri M; Bello D; Pal AK; Cohen JM; Woskie S; Gassert T; Lan J; Gu AZ; Demokritou P; Gaines P, Evaluation of cytotoxic, genotoxic and inflammatory responses of nanoparticles from photocopiers in three human cell lines. *Particle and Fibre Toxicology* 2013, 10, (1), 42. [PubMed: 23968360]
57. Vandesompele J; De Preter K; Pattyn F; Poppe B; Van Roy N; De Paepe A; Speleman F, Accurate normalization of real-time quantitative RT-PCR data by geometric averaging of multiple internal control genes. *Genome biology* 2002, 3, (7), research0034. 1.
58. Schmittgen TD; Livak KJ, Analyzing real-time PCR data by the comparative C T method. *Nature Protocols* 2008, 3, (6), 1101. [PubMed: 18546601]
59. De Brouwere K; Cornelis C; Arvanitis A; Brown T; Crump D; Harrison P; Jantunen M; Price P; Torfs R, Application of the maximum cumulative ratio (MCR) as a screening tool for the evaluation of mixtures in residential indoor air. *Science of the Total Environment* 2014, 479, 267–276.
60. Reyes JM; Price PS, An analysis of cumulative risks based on biomonitoring data for six phthalates using the Maximum Cumulative Ratio. *Environment International* 2018, 112, 77–84. [PubMed: 29253731]
61. Vallotton N; Price PS, Use of the maximum cumulative ratio as an approach for prioritizing aquatic coexposure to plant protection products: A case study of a large surface water monitoring database. *Environmental Science & Technology* 2016, 50, (10), 5286–5293. [PubMed: 27057923]
62. Zhang X; Lohmann R; Dassuncao C; Hu XC; Weber AK; Vecitis CD; Sunderland EM, Source attribution of poly- and perfluoroalkyl substances (PFASs) in surface waters from Rhode Island and the New York Metropolitan Area. *Environ Sci Technol Lett* 2016, 3, (9), 316–321. [PubMed: 28217711]
63. Akman O; Comar T; Hrozencik D; Gonzales J, Chapter 11 - Data Clustering and Self-Organizing Maps in Biology In *Algebraic and Combinatorial Computational Biology*, Robeva R; Macauley M, Eds. Academic Press: 2019; pp 351–374.
64. Escher BI; Allinson M; Altenburger R; Bain PA; Balaguer P; Busch W; Crago J; Denslow ND; Dopp E; Hilscherova K; Humpage AR; Kumar A; Grimaldi M; Jayasinghe BS; Jarosova B; Jia A; Makarov S; Maruya KA; Medvedev A; Mehinto AC; Mendez JE; Poulsen A; Prochazka E; Richard J; Schifferli A; Schlenk D; Scholz S; Shiraishi F; Snyder S; Su G; Tang JY; van der Burg B; van der Linden SC; Werner I; Westerheide SD; Wong CK; Yang M; Yeung BH; Zhang X; Leusch FD, Benchmarking organic micropollutants in wastewater, recycled water and drinking water with in vitro bioassays. *Environ Sci Technol* 2014, 48, (3), 1940–56. [PubMed: 24369993]
65. Andrade-Eiroa A; Canle M; Leroy-Cancellieri V; Cerda V, Solid-phase extraction of organic compounds: A critical review (Part I). *Trac-Trends in Analytical Chemistry* 2016, 80, 641–654.
66. Andrade-Eiroa A; Canle M; Leroy-Cancellieri V; Cerda V, Solid-phase extraction of organic compounds: A critical review. *Trac-Trends in Analytical Chemistry* 2016, 80, 655–667.

67. Davis AP; Grondin CJ; Johnson RJ; Sciaky D; King BL; McMorran R; Wiegers J; Wiegers TC; Mattingly CJ, The comparative toxicogenomics database: update 2017. *Nucleic Acids Research* 2016, 45, (D1), D972–D978. [PubMed: 27651457]
68. Mattingly CJ; Colby GT; Forrest JN; Boyer JL, The Comparative Toxicogenomics Database (CTD). *Environmental Health Perspectives* 2003, 111, (6), 793–795. [PubMed: 12760826]
69. Stackelberg PE; Furlong ET; Meyer MT; Zaugg SD; Henderson AK; Reissman DB, Persistence of pharmaceutical compounds and other organic wastewater contaminants in a conventional drinking-water-treatment plant. *Science of the Total Environment* 2004, 329, (1–3), 99–113.
70. Costanzo S; Watkinson A; Murby E; Kolpin DW; Sandstrom MW, Is there a risk associated with the insect repellent DEET (N, N-diethyl-m-toluamide) commonly found in aquatic environments? *Science of the Total Environment* 2007, 384, (1-3), 214–220.
71. Sudakin DL; Trevathan WR, DEET: a review and update of safety and risk in the general population. *Journal of Toxicology: Clinical Toxicology* 2003, 41, (6), 831–839. [PubMed: 14677793]
72. Abou-Donia M, Neurotoxicity resulting from coexposure to pyridostigmine bromide, DEET, and permethrin: implications of Gulf War chemical exposures. *Journal of Toxicology and Environmental Health* 1996, 48, (1), 35–56. [PubMed: 8637057]
73. Tisch M; Schmezer P; Faulde M; Groh A; Maier H, Genotoxicity studies on permethrin, DEET and diazinon in primary human nasal mucosal cells. *European Archives of Otorhino-laryngology* 2002, 259, (3), 150–153.
74. Billet S; Abbas I; Le Goff J; Verdin A; André V; Lafargue P-E; Hachimi A; Cazier F; Sichel F; Shirali P, Genotoxic potential of polycyclic aromatic hydrocarbons-coated onto airborne particulate matter (PM_{2.5}) in human lung epithelial A549 cells. *Cancer Letters* 2008, 270, (1), 144–155. [PubMed: 18554780]
75. Hukkanen J; Lassila A; Paivarinta K; Valanne S; Sarpo S; Hakkola J; Pelkonen O; Raunio H, Induction and regulation of xenobiotic-metabolizing cytochrome P450s in the human A549 lung adenocarcinoma cell line. *American Journal of Respiratory Cell and Molecular Biology* 2000, 22, (3), 360–366. [PubMed: 10696073]
76. Iwanari M; Nakajima M; Kizu R; Hayakawa K; Yokoi T, Induction of CYP1A1, CYP1A2, and CYP1B1 mRNAs by nitropolycyclic aromatic hydrocarbons in various human tissue-derived cells: chemical-, cytochrome P450 isoform-, and cell-specific differences. *Archives of Toxicology* 2002, 76, (5-6), 287–298. [PubMed: 12107646]
77. Li S; He B; Wang J; Liu J; Hu X, Risks of caffeine residues in the environment: Necessity for a targeted ecopharmacovigilance program. *Chemosphere* 2020, 243, 125343. [PubMed: 31751929]
78. Mateo-Fernandez M; Merinas-Amo T; Moreno-Millan M; Alonso-Moraga A; Demyda-Peyras S, In Vivo and In Vitro Genotoxic and Epigenetic Effects of Two Types of Cola Beverages and Caffeine: A Multiassay Approach. *Biomed Research International* 2016, 15.
79. Quinones-Gonzalez CA; Arredondo-Mendoza GI; Jimenez-Salas Z; Larriba-Calle G; Ruiz-Herrera J; Campos-Gongora E, Genotoxic effect of caffeine in *Yarrowia lipolytica* cells deficient in DNA repair mechanisms. *Arch. Microbiol.* 2019, 201, (7), 991–998. [PubMed: 31025056]
80. Selby CP; Sancar A, Molecular mechanisms of DNA-repair inhibition by caffeine. *Proceedings of the National Academy of Sciences of the United States of America* 1990, 87, (9), 3522–3525. [PubMed: 2185474]
81. Eriksen KT; Raaschou-Nielsen O; Sorensen M; Roursgaard M; Loft S; Moller P, Genotoxic potential of the perfluorinated chemicals PFOA, PFOS, PFBS, PFNA and PFHxA in human HepG2 cells. *Mutation research* 2010, 700, (1–2), 39–43. [PubMed: 20451658]
82. Panaretakis T; Shabalina IG; Grandier D; Shoshan MC; DePierre JW, Reactive oxygen species and mitochondria mediate the induction of apoptosis in human hepatoma HepG2 cells by the rodent peroxisome proliferator and hepatocarcinogen, perfluorooctanoic acid. *Toxicology and applied pharmacology* 2001, 173, (1), 56–64. [PubMed: 11350215]
83. Yao X; Zhong L, Genotoxic risk and oxidative DNA damage in HepG2 cells exposed to perfluorooctanoic acid. *Mutation research* 2005, 587, (1–2), 38–44. [PubMed: 16219484]
84. Kamendulis LM; Wu Q; Sandusky GE; Hocesvar BA, Perfluorooctanoic acid exposure triggers oxidative stress in the mouse pancreas. *Toxicology reports* 2014, 1, 513–521. [PubMed: 28962265]

85. Li K; Gao P; Xiang P; Zhang X; Cui X; Ma LQ, Molecular mechanisms of PFOA-induced toxicity in animals and humans: Implications for health risks. *Environ Int* 2017, 99, 43–54. [PubMed: 27871799]
86. Tsuda S, Differential toxicity between perfluorooctane sulfonate (PFOS) and perfluorooctanoic acid (PFOA). *The Journal of toxicological sciences* 2016, 41, (Special), Sp27–sp36. [PubMed: 28003637]
87. Arbelález P; Borrull F; Pocurull E; Marcé RM, Determination of high-intensity sweeteners in river water and wastewater by solid-phase extraction and liquid chromatography–tandem mass spectrometry. *Journal of Chromatography A* 2015, 1393, 106–114. [PubMed: 25840659]
88. Lange FT; Scheurer M; Brauch H-J, Artificial sweeteners—a recently recognized class of emerging environmental contaminants: a review. *Analytical and Bioanalytical Chemistry* 2012, 403, (9), 2503–2518. [PubMed: 22543693]
89. Loos R; Carvalho R; António DC; Comero S; Locoro G; Tavazzi S; Paracchini B; Ghiani M; Lettieri T; Blaha L, EU-wide monitoring survey on emerging polar organic contaminants in wastewater treatment plant effluents. *Water Research* 2013, 47, (17), 6475–6487. [PubMed: 24091184]
90. Cruz-Rojas C; SanJuan-Reyes N; Fuentes-Benites MPAG; Dublan-García O; Galar-Martínez M; Islas-Flores H; Gómez-Oliván LM, Acesulfame potassium: Its ecotoxicity measured through oxidative stress biomarkers in common carp (*Cyprinus carpio*). *Science of the Total Environment* 2019, 647, 772–784.
91. Saucedo-Vence K; Elizalde-Velazquez A; Dublan-Garcia O; Galar-Martinez M; Islas-Flores H; SanJuan-Reyes N; Garcia-Medina S; Hernandez-Navarro MD; Gomez-Olivan LM, Toxicological hazard induced by sucralose to environmentally relevant concentrations in common carp (*Cyprinus carpio*). *The Science of the total environment* 2017, 575, 347–357. [PubMed: 27744200]
92. Kim J-Y; Park K-H; Kim J; Choi I; Cho K-H, Modified high-density lipoproteins by artificial sweetener, aspartame, and saccharin, showed loss of anti-atherosclerotic activity and toxicity in zebrafish. *Cardiovascular Toxicology* 2015, 15, (1), 79–89. [PubMed: 25142179]
93. Eriksson Wiklund AK; Adolfsen-Erici M; Liewenborg B; Gorokhova E, Sucralose induces biochemical responses in *Daphnia magna*. *PLoS One* 2014, 9, (4), e92771. [PubMed: 24699280]
94. Price PS; Han X, Maximum cumulative ratio (MCR) as a tool for assessing the value of performing a cumulative risk assessment. *International Journal of Environmental Research and Public Health* 2011, 8, (6), 2212–2225. [PubMed: 21776227]
95. Toccalino P, Development and application of health-based screening levels for use in water-quality assessments. Citeseer: 2007.
96. Toccalino P; Rowe BL; Norman JE, Volatile Organic Compounds in the Nation's Drinking-water Supply Wells: What Findings May Mean to Human Health. US Department of the Interior, US Geological Survey: 2006.
97. United States Environmental Protection Agency, Technical fact sheet-Perfluorooctane Sulfonate (PFOS) and Perfluorooctanoic Acid (PFOA). EPA 505-F-17-001. Office of Land and Emergency Management In 2017.
98. Teaf CM; Garber MM; Covert DJ; Tuovila BJ, Perfluorooctanoic Acid (PFOA): Environmental Sources, Chemistry, Toxicology, and Potential Risks. *Soil and Sediment Contamination: An International Journal* 2019, 28, (3), 258–273.

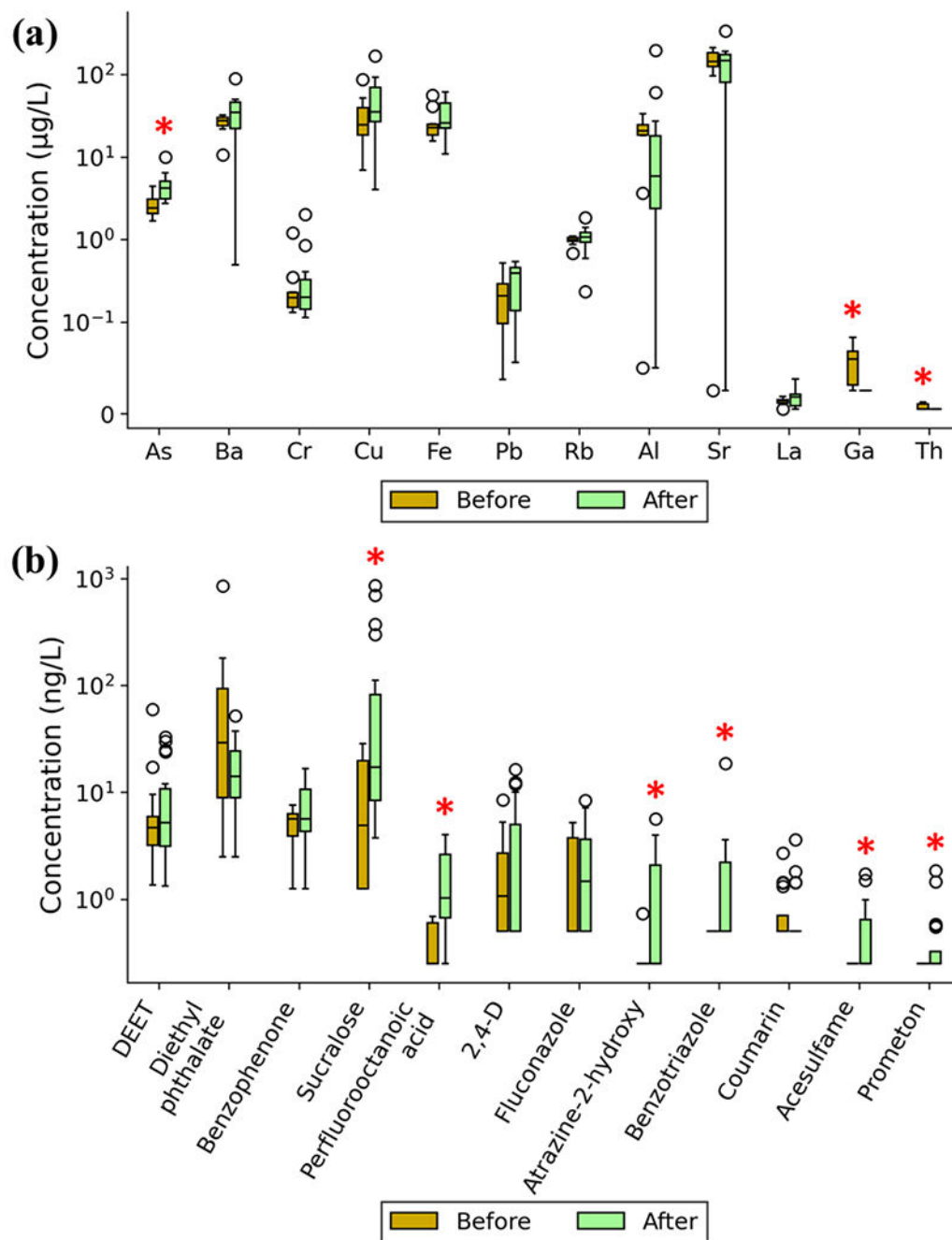


Figure 1.

Box plots showing concentration statistics of top 10 frequently detected (a) trace elements, (b) organic micropollutants and those showed significant ($p < 0.05$) changes after Hurricane Maria (HM) in the tap water samples collected at Puerto Rico. The black line within each box is the median with box top and bottom as 75th percentile and 25th percentile, respectively. The maximum observation (after removal of outliers) and minimum value are also shown. Outliers are defined based on the interquartile range (IQR) rule. Those

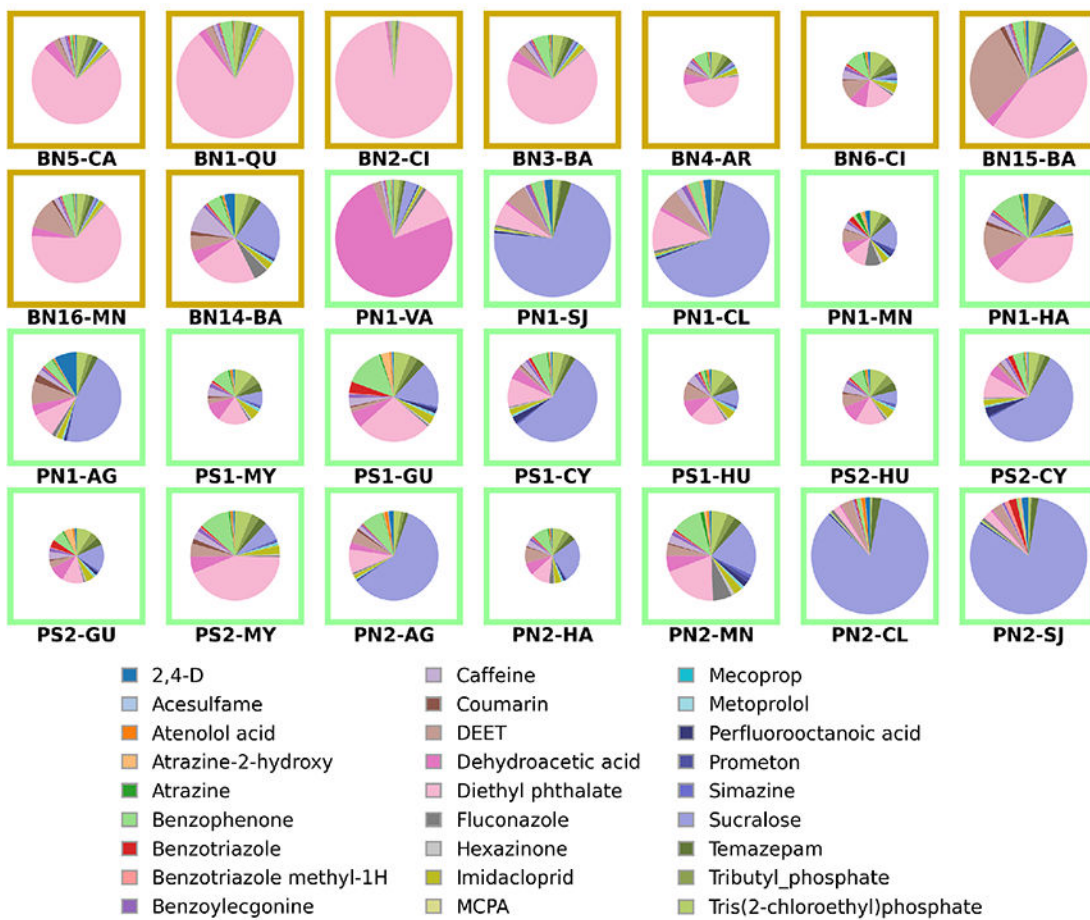
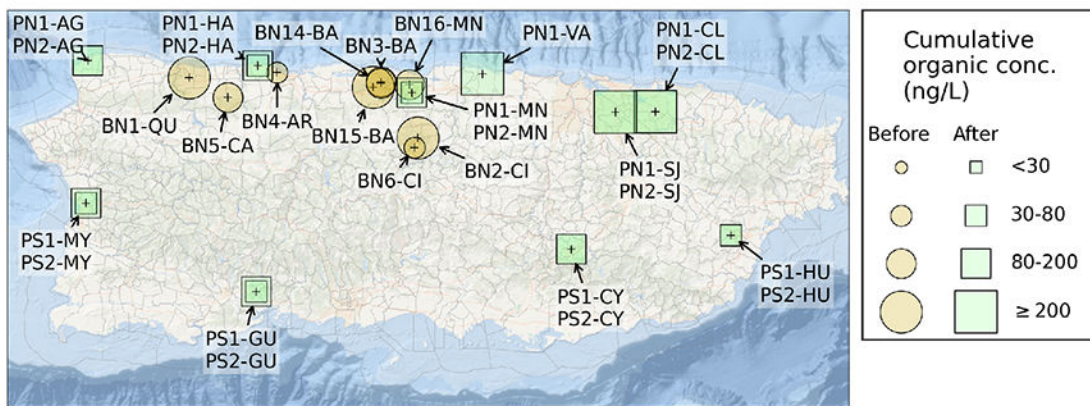
contaminants highlighted with red asterisks (*) showed significant ($p < 0.05$) difference in their concentrations before and after HM in both unpaired t-test and MWU test.

Author Manuscript

Author Manuscript

Author Manuscript

Author Manuscript



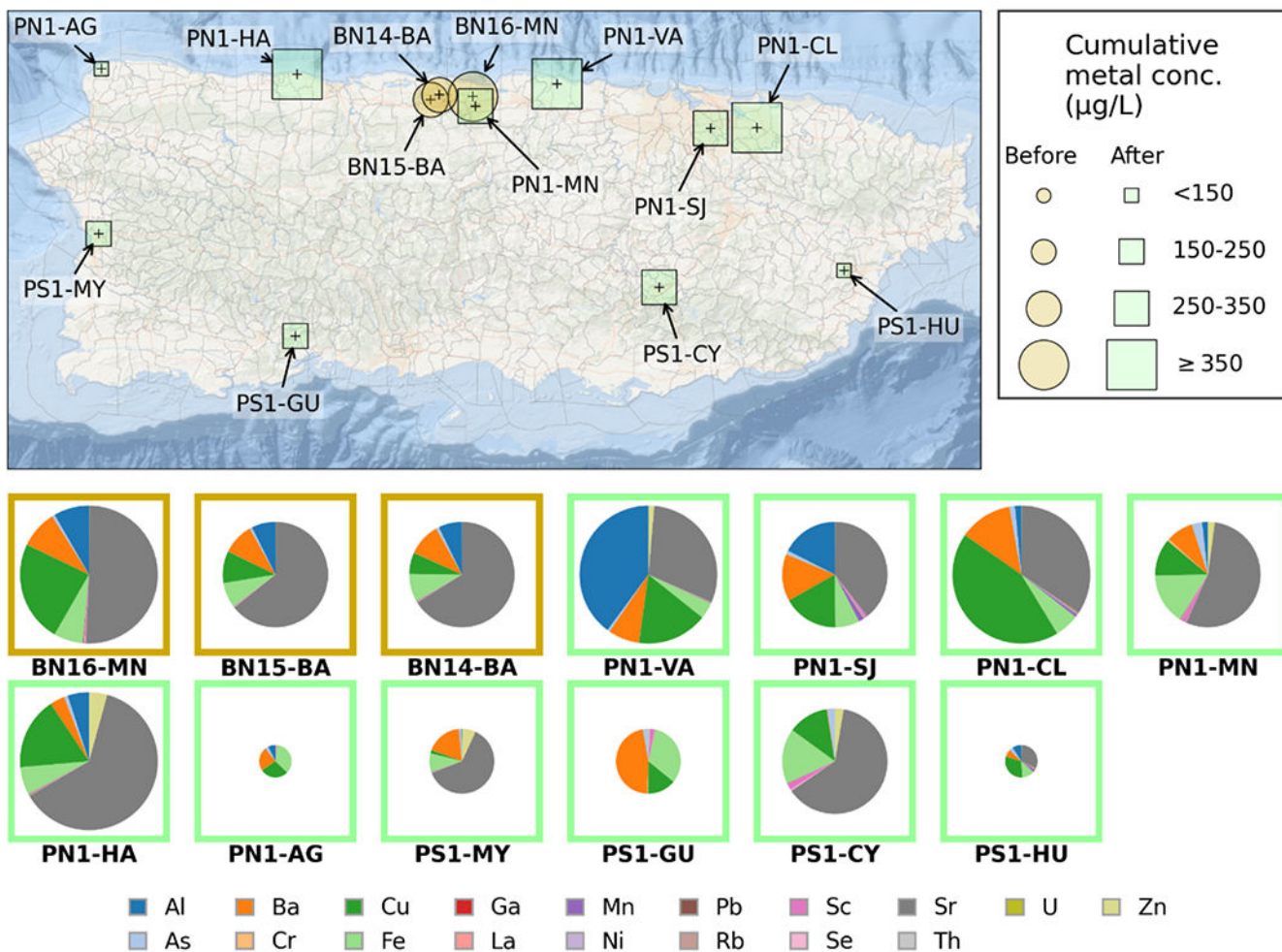


Figure 2. Top: Cumulative concentration of detected trace elements in raw tap water samples collected at different sampling locations in Puerto Rico measured via ICP-MS, before and after Hurricane Maria (Top); and percentage distribution of element concentration in each tap water sample for before-HM samples (orange square) and post-HM sample (green square) (Bottom pie charts). Bottom: Cumulative concentration of detected organic micropollutants in tap water samples collected at different sampling locations in Puerto Rico, before and after Hurricane Maria (Top); and percentage distribution of micropollutants concentration in each tap water sample extract for before-HM samples (orange square) and post-HM sample (green square) (Bottom pie charts).

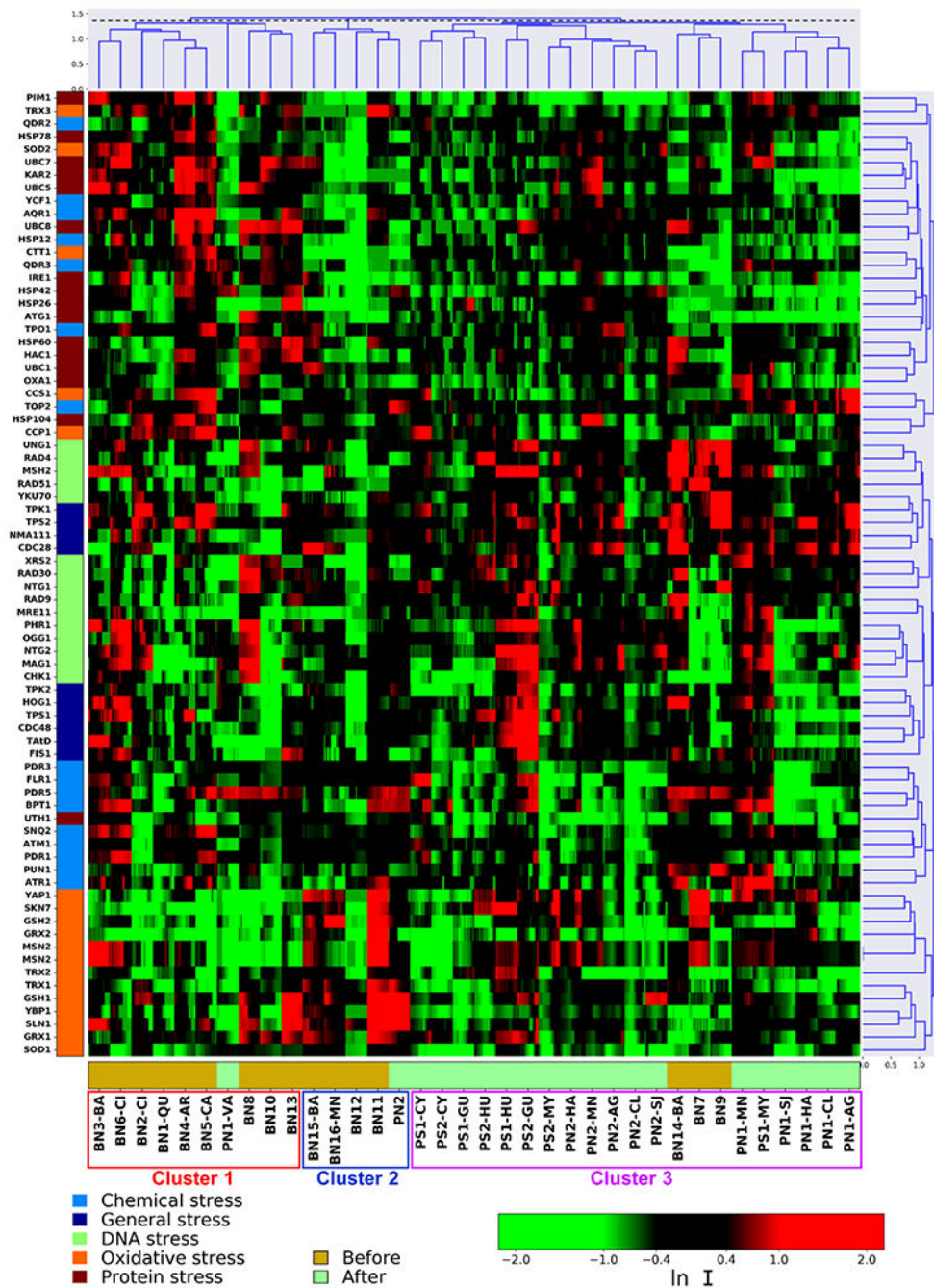


Figure 3. Hierarchical clustering analysis (HCA) diagram on the basis of differential protein expressions (average $\ln I$) of the 74 stress biomarkers in yeast strains in exposure to tap water extracts (REF=200) across Puerto Rico before and after Hurricane Maria. The mean natural log of positive induction factors ($\ln I$) indicate the magnitude of altered protein expression (scaled by the green-black-red color spectrum). Green color spectrum indicates down-regulation compared to the untreated control without chemical dosage, and red color indicates up-regulation. The $\ln I$ values beyond ± 2 were indicated as ± 2 . X-axis top: cluster

root of the samples that was cut (dashed line) to present three main clusters. X-axis bottom: sample names color-coded according to time-lines: before HM (light yellow) and after HM (light green). Y-axis left: list of proteins color-coded based on the five stress categories (Table S4). Y-axis right: cluster root of stress response-related proteins.

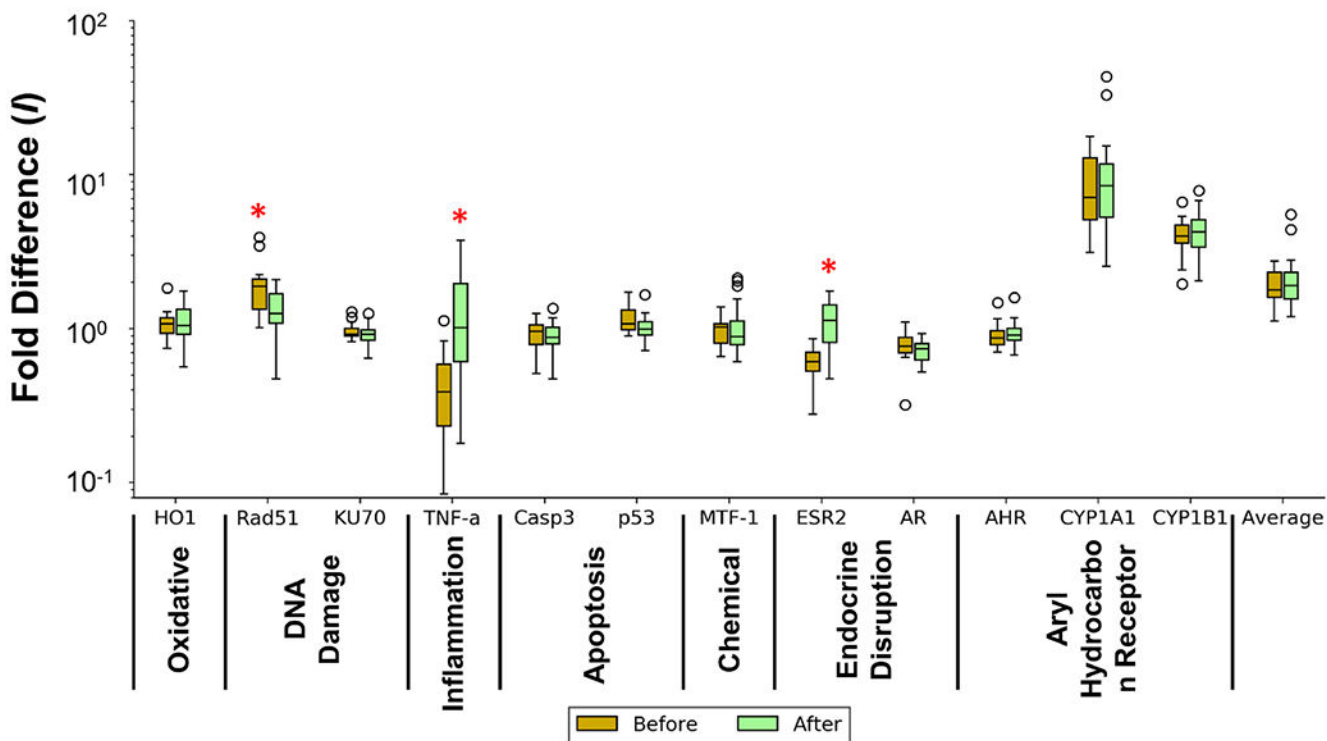


Figure 4. Box plots showing statistics of fold difference (J) of 12 biomarkers in human A549 cell upon exposure to tap water samples collected at Puerto Rico before and after Hurricane Maria (HM) based on RT-qPCR assay. The black line within each box is the median with box top and bottom as 75th percentile and 25th percentile, respectively. The maximum observation (after removal of outliers) and minimum value are also shown. Outliers are defined based on the interquartile range (IQR) rule. A red asterisk (*) shows a biomarker in human cells that was significantly different ($p < 0.05$) in the samples before and after HM in both t-test and MWU test.

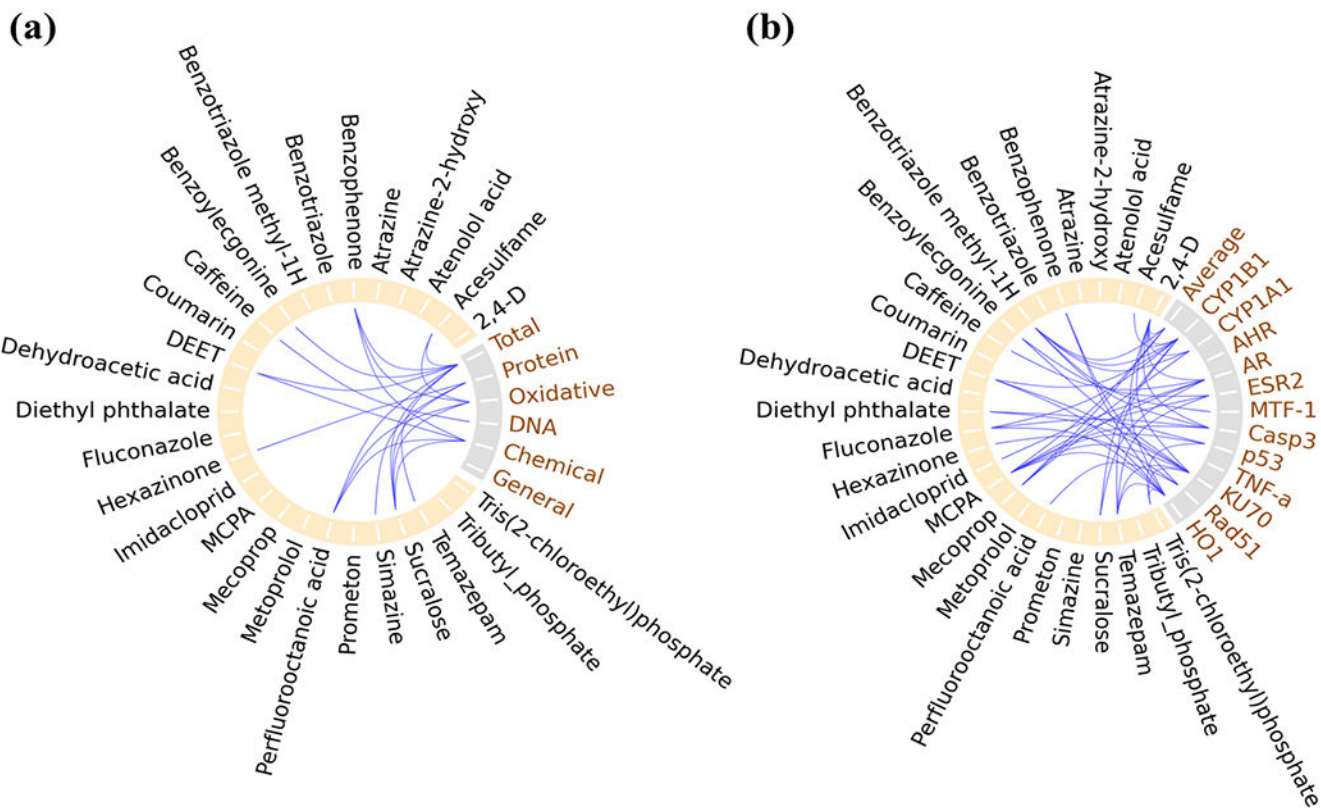


Figure 5. Pearson correlation analysis between organic micropollutant content in the 36 tap water extracts and molecular toxicity quantifiers of (a) different stress response categories in yeast library or (b) human biomarkers. Lines connecting two parameters indicating significant correlation between the two ($p < 0.05$).

Table 1.

Hazard index (HI), maximum cumulative ratio (MCR), and top-ranked high-priority substances in the twenty-one tap water samples collected at Puerto Rico (PR) ^a.

Sample ID	HI	HQ _{max}	MCR	Top 5 High-Priority Substances (HQ from high to low)
BN7	0.4260	0.2056	2.0721	As, Fe, Sr, Cu, Pb
BN8	0.3498	0.2089	1.6744	As, Fe, Sr, Ba, PFOA
BN9	0.3143	0.1748	1.7979	As, Fe, Sr, Cu, Ba
BN10	0.3164	0.1678	1.8854	As, Fe, Sr, Cu, Ba
BN11	0.5733	0.3302	1.7361	As, Fe, Cu, U, Pb
BN12	0.5954	0.4439	1.3412	As, Fe, Sr, Pb, Ba
BN13	0.7416	0.4166	1.7804	As, Fe, U, Pb, Sr
BN14-BA	0.4411	0.2480	1.7785	As, Fe, Sr, Pb, Cu
BN15-BA	0.4667	0.2458	1.8982	As, Fe, Sr, Cu, Ba
BN16-MN	0.5037	0.2367	2.1278	As, Fe, Cu, Sr, Pb
PN1-VA	0.5213	0.2770	1.8819	As, Cu, Fe, Sr, Al
PN2	0.5263	0.2754	1.9107	As, Fe, Sr, Ni, Pb
PN1-SJ	0.7110	0.4206	1.6903	As, Fe, PFOA, Cu, Sr
PN1-CL	0.8349	0.4912	1.6998	As, Cu, Fe, PFOA, Sr
PN1-MN	1.3403	0.9914	1.3520	As, Fe, Sr, Pb, Cu
PN1-HA	0.8359	0.4801	1.7411	As, Fe, Sr, Cu, Pb
PN1-AG	0.6382	0.4054	1.5742	As, Fe, Cu, U, PFOA
PS1-MY	0.4576	0.3011	1.5200	As, Fe, Sr, Ba, Zn
PS1-GU	0.8760	0.5339	1.6407	As, Fe, Ba, Cu, PFOA
PS1-CY	1.0016	0.6448	1.5534	As, Fe, Sr, PFOA, Pb
PS1-HU	0.4242	0.3202	1.3248	As, Fe, Pb, Cu, Sr

^a: HI, HQ_{max}, and MCR values were calculated based on selected human-health benchmarks as indicated in Table S11.